Terahertz imaging with quantum cascade lasers

Citation: Lee, Alan W. et al. "Terahertz Imaging with Quantum Cascade Lasers." Proceedings Volume 9854: Image Sensing Technologies: Materials, Devices, Systems, and Applications III, 17-21 April, 2016, Baltimore, Maryland, edited by Nibir K. Dhar and Achyut K. Dutta, SPIE, 2016, pp. 9629–9653 © 2016 Society of Photo-Optical Instrumentation Engineers (SPIE)

As Published: http://dx.doi.org/10.1117/12.2224140

Publisher: SPIE

Persistent URL: http://hdl.handle.net/1721.1/114213

Version: Final published version: final published article, as it appeared in a journal, conference proceedings, or other formally published context

Terahertz imaging with quantum cascade lasers

Alan W. Lee, Tsung-Yu Kao, Ian A. Zimmerman, Naoki Oda, Qing Hu

Alan W. Lee, Tsung-Yu Kao, Ian A. Zimmerman, Naoki Oda, Qing Hu, "Terahertz imaging with quantum cascade lasers," Proc. SPIE 9854, Image Sensing Technologies: Materials, Devices, Systems, and Applications III, 98540R (26 May 2016); doi: 10.1117/12.2224140

SPIE.

Event: SPIE Commercial + Scientific Sensing and Imaging, 2016, Baltimore, Maryland, United States

Terahertz Imaging with Quantum Cascade Lasers

Alan W. Lee*[a], Tsung-Yu Kao [a], Ian A. Zimmerman [a], Naoki Oda[b]; Qing Hu[c]
[a] LongWave Photonics LLC, 958 San Leandro Ave, Mountain View, CA, USA 94043; [b] NEC Corporation, Radio Applications, Guidance and Electro-Optics Division; [c]Massachusetts Institute of Technology, Cambridge, MA 02139

ABSTRACT

Milliwatt average power terahertz quantum cascade lasers (THz-QCLs) combined with microbolometer focal plane array cameras allow for acquisition rates on the order of 1×10^6 pixels/s. This system enables real-time imaging in transmission and reflection modes with signal to noise ratios of >25 dB per pixel. While these system allow rapid imaging for fairly transparent samples, signal to noise ratios of > 90 dB can be achieved with single element detectors where the samples are more opaque or require higher SNR. Systems using LongWave's terahertz QCLs and single/multi-element detectors will be presented.

Keywords: terahertz quantum cascade laser, spectroscopy, heterodyne

1. INTRODUCTION

Non-destructive evaluation (NDE) applications are among the most promising for the terahertz spectral region (1 to 10 THz) because it allows operator safe, non-contact measurement of materials that would otherwise be opaque to visible and infrared frequencies: polymers, ceramics, semiconductors and electrical insulators. Existing terahertz NDE equipment is relatively complex because the terahertz radiation is generated by indirect means, through optical down conversion from the infrared; this may limit the cost reduction potential of this technology and its ability to compete with existing NDE technologies such as ultrasound, eddy current meters, infrared imaging, and x-ray imaging. Terahertz Quantum-Cascade Laser (QCL) sources show promise as a compact, easy to use source of light from 2 to 5 THz as these semiconductor lasers have no moving parts and have demonstrated power levels of >1 W [1], with maximum operating temperatures of 200 K [2]. The relatively high powers make these sources compatible with room temperature direct detector arrays [3-4].

In this paper we present turnkey THz QCL systems for investigation of NDE applications. We also present a real-time imaging systems for NDE, as well as a thickness measurement system using laser triangulation. Lastly we present a single pixel confocal system for scanned imaging.

*awmlee@longwavephotonics.com; phone 617 399 6405; fax 617 399 6406; www.longwavephotonics.com

Image Sensing Technologies: Materials, Devices, Systems, and Applications III, edited by Nibir K. Dhar, Achyut K. Dutta, Proc. of SPIE Vol. 9854, 98540R · © 2016 SPIE · CCC code: 0277-786X/16/$18 · doi: 10.1117/12.2224140

2. TURNKEY THZ QCL SYSTEMS

The THz QCL gain media used in this work is based on the resonant phonon gain medium design [5]. Devices fabricated into metal-metal waveguide [6] have shown the best temperature performance, but have highly divergent beam patterns exceeding 180°. To compensate for this, we attach an integrated microlens (as shown in Figure 1)[7]. Typical device characteristics at an operating in Figure 1. Here the device is operated in continous wave with an output power of > 6 mW with a symmetrical beam pattern and electrical power consumption of 2.4 W (0.25% wall plug efficiency at 47 K).

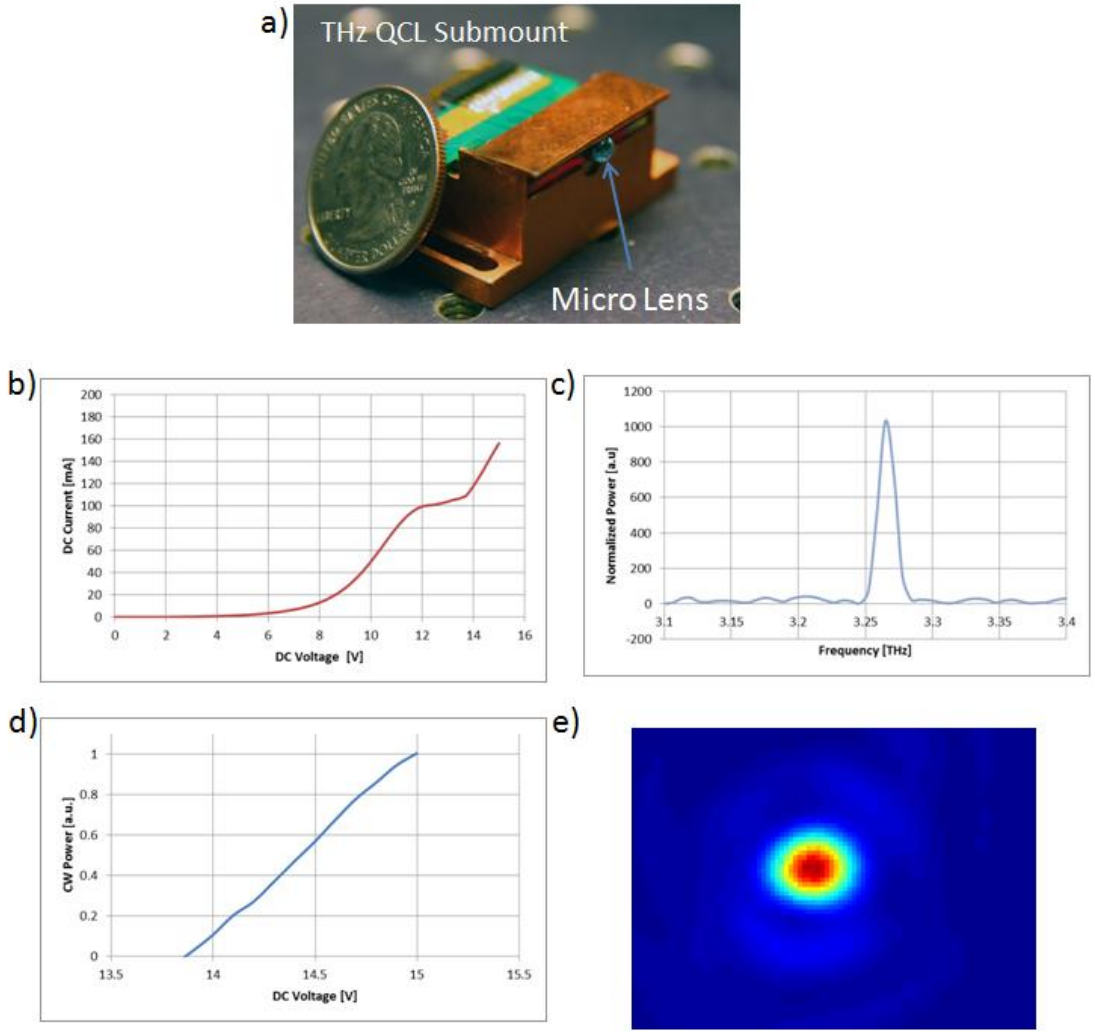

Figure 1 Part (a) QCL subassembly with integrated microlens attached to QCL. Lens is high-resistivity silicon anti-reflection coated for 3.2 THz using Parylene. Part (b) shows current versus voltage characteristic of device. Part (c) shows emission spectra of device. Part (d) shows light versus voltage characteristic. Part (e) shows focused beam pattern using 25.4 mm f/1 lens and NEC IRV-T0831 camera.

To facilitate rapid prototyping of imaging systems, several cryogen-free cryocooler systems have been developed as shown in. Part (a) shows a larger system based on the Cryomech PT63 pulse tube

cooler, which can be used with devices with higher electrical power dissipation (and higher optical output powers). The no-load temperature of this system is typically 22 K, and the cold stage increases temperature at 0.8 K per watt of power dissipation -- therefore a large device dissipating 15 W, can be adequately cooled and remain ~34 K. At this temperature there is small (<10%) power output difference compared with operation at 22 K. The large heat lift capability of this system is often not required, and a smaller system based a smaller cooler with an integral compressor is shown in part (b). This system is light (<12 kg), operates with less than 250 W DC power, in a 48 × 22 × 17 cm^3 form factor for convenient laboratory use. Here the no-load temperature is approximately 35 K with temperature increase of 3.2 K/W. For a device such as that shown in Figure 1, a temperature of 47 K can be maintained in closed loop +/- 0.1at For flexibility, QCLs are interchangeable and a variety of QCLs are available between 2 and 5 THz in multi-mode Fabry-Perot devices, and well as single mode DFB devices

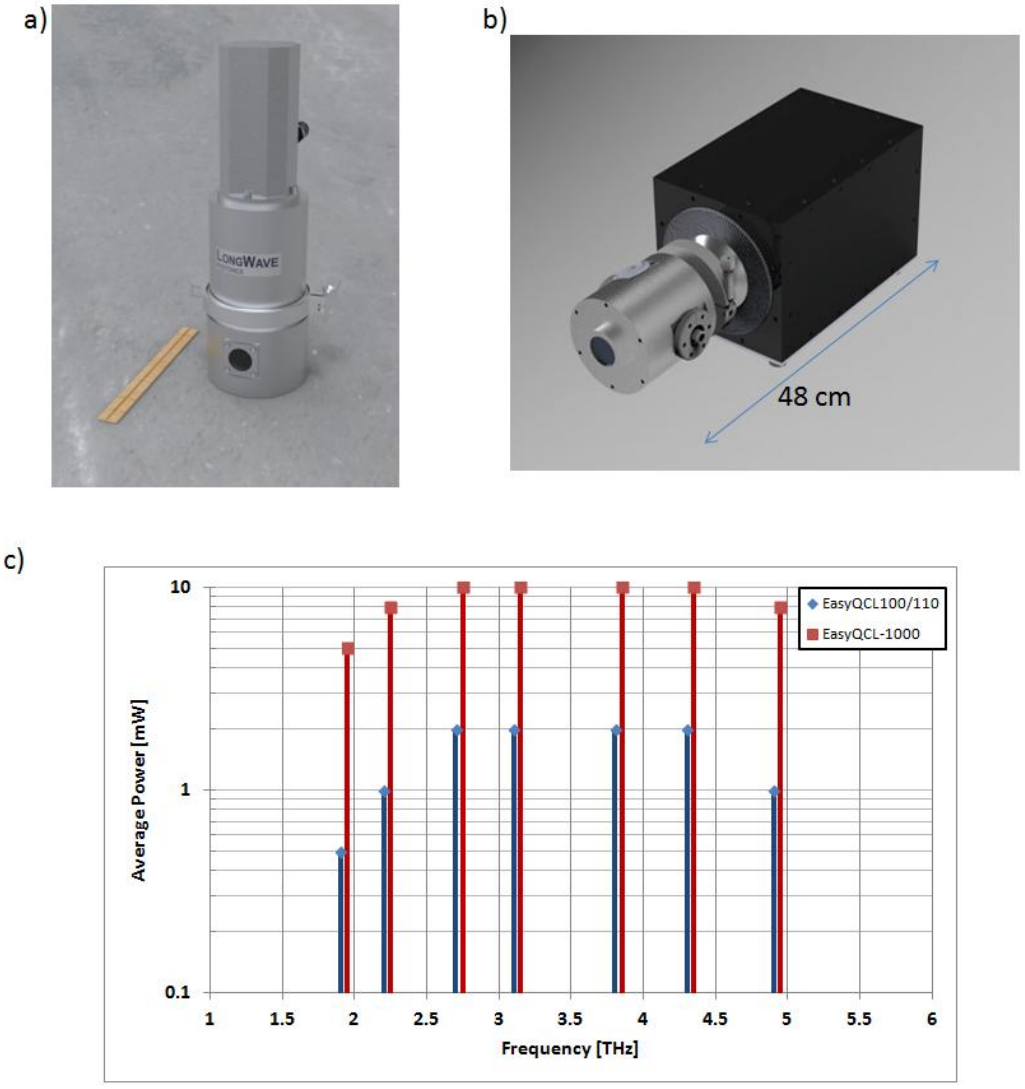

Figure 2: Approximate footprint of larger (a) and smaller closed cycle crycooler systems shown. Part (c) shows various Fabry-Perot lasers and their minimum average output powers in the larger

3. IMAGING WITH THZ QCLS

3.1 Real-Time Terahertz Imaging with a microbolometer focal-plane array

To demonstrate the feasibility of a compact NDE system for defects in plastic, a prototype microscope system was assembled from the EasyQCL-110 as shown in Figure 3. A sample application would be for the inspection of defects in a plastic ultrasonic weld. Here a 4.3 THz QCL is operated at 47 K with a bias of 418 mA and 14.5 emitted an average power 2.2 mW at 25% duty cycle (100 kHz, 2.5 µs). The output beam is collimated with a 25.4 mm f/1 high-resistivity silicon lens resulting in a beam diameter of < 10 mm. Using 2-axis galvo scanner as implemented in [8], the beam is raster scanned over the sample stage using a predetermined scan pattern (parts c and d). An imaging lens (25.4 mm f/1 high-resistivity silicon) is used to focus THz light onto a microbolometer focal plane array (NEC, IRV-T0831). Here the galvo scan patterns are scanned at > 100 Hz to minimize aliasing with the 30 Hz acquisition rate of the camera. The resulting scan patterns are seen in parts e and f. A 6.35-mm thick high-density polyethylene sheet with a scratch pattern (part g, visible) was manually scanned across the screen (video online). The ~100-µm wide scratch is clearly visible at THz wavelengths.

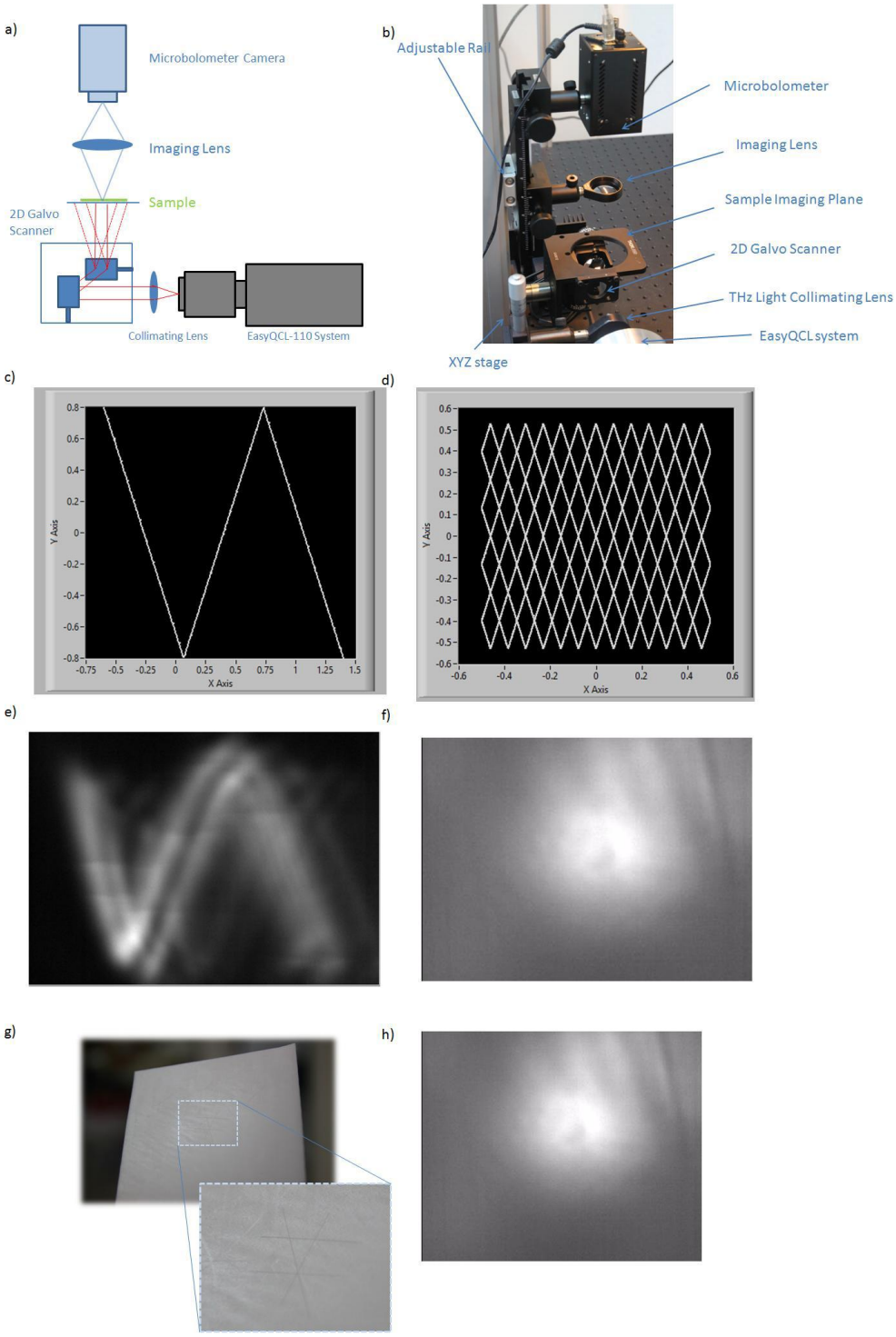

Figure 3: Part (a) shows schematic real-time imaging system with imaging in part (b). Imaging system uses galvo scanner to homogenize the QCL beam over the object. Parts (c)/(d) show simple/complex scan patterns of galvo scanner, with THz images shown in parts (e) and (f). Part (g) shows image of HDPE plastic with scratches and part (h) shows a single frame of THz video of plastic (http://dx.doi.org/10.1117/12.2224140.1).

3.2 Laser triangulation depth measurement

Depth measurement or range finding by laser triangulation is commonly used in industry for the micron level depth accuracy, mechanical robustness and real-time speed [9-11]. Typically the collimated light from a visible or near infrared laser is reflected off the top surface of an object and imaged onto a CCD array. As the beam is scanned over the object, differences in the object height result in a change in position of the signal on the CCD. For a transparent object, light can be reflected off the interfaces within the object, and measurement can take place in specular (Figure 4 part a) or diffuse (part b) reflectance mode [12]. Laser triangulation allows depth information to be converted to lateral position information on the CCD.

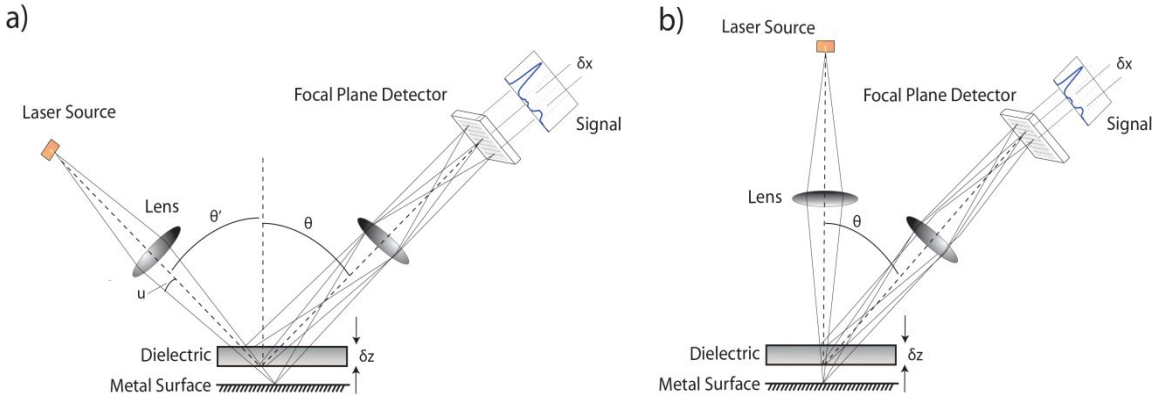

Figure 4: Laser triangulation in specular reflection (a) and diffuse reflection (b) configurations. In both configurations reflections from dielectric/metal interfaces are imaged to distinct positions on focal plane array. A single line of the array ('Signal') is used to calculate the relative positions of the interfaces.

Diffuse reflectance mode is preferable because it relies on light scatter from the rough surface of the object, allowing nearly independent positioning of the laser with respect to the CCD. This allows the laser beam to be angularly scanned at video rates over the surface of the object, which can remain stationary [13]. In the case where the surface roughness of the object is not sufficient for diffuse imaging, the specular configuration can obtain 3D imagery by raster scanning of the object or the laser/detector.

The depth resolution (δz) of a laser triangulation system is limited by the beam waist (ω_o) on the surface of the object [14]:

Eq 1
$$\delta z \approx \frac{\omega_o}{2 \cdot \sin\theta} = \frac{1}{2\pi} \cdot \frac{\lambda}{\sin u} \cdot \frac{1}{\sin\theta}$$

For a Gaussian beam the beam waist is $\omega_o = \lambda/\pi \cdot \sin u$, where λ is the wavelength of light, u is the angle of convergence of the laser beam incident on the surface and θ is the observing angle of the detector with respect to the surface normal. Laser triangulation clearly favors shorter wavelengths

and larger observation angles. For optimized systems δz can be on the order of several wavelengths (~2 λ) [10, 14].

Laser triangulation based 3D imaging is shown in Figure 5. The prototype system uses a 4.3 THz QCL mounted in a closed cycle, cryorefrigerator, which cools the device to 30 K. The device emits a peak power of 50 mW at 15% duty cycle in 13.5 ms long pulses as described in [15]. The beam emitted from the QCL is collected by off-axis parabolic mirrors and is focused through an aperture to form a near diffraction-limited beam. The beam is focused with a 50 mm silicon optic so that the beam waist is approximately at the sample, which consists of a 3.2-mm thick high-density polyethylene (HDPE) sheet, separated by a variable distance from a metal reflecting surface. Due to the smooth surfaces of the polyethylene and metal layers, and the low sensitivity (NEP≈320 pW/√Hz) of the microbolometer detector array, only specular reflections were obtainable. The specular reflection from the top interface (air/HDPE), bottom interface (HDPE/air), and metal layer are clearly visible in real-time as laterally displaced images of the beam waist. A plot of a single row from the microbolometer array allows the distances between the surfaces to be measured if the index of refraction of HDPE is known (n≈1.5). The minimum resolvable separation between the metal surface and the HDPE sheet was ~250 μm.

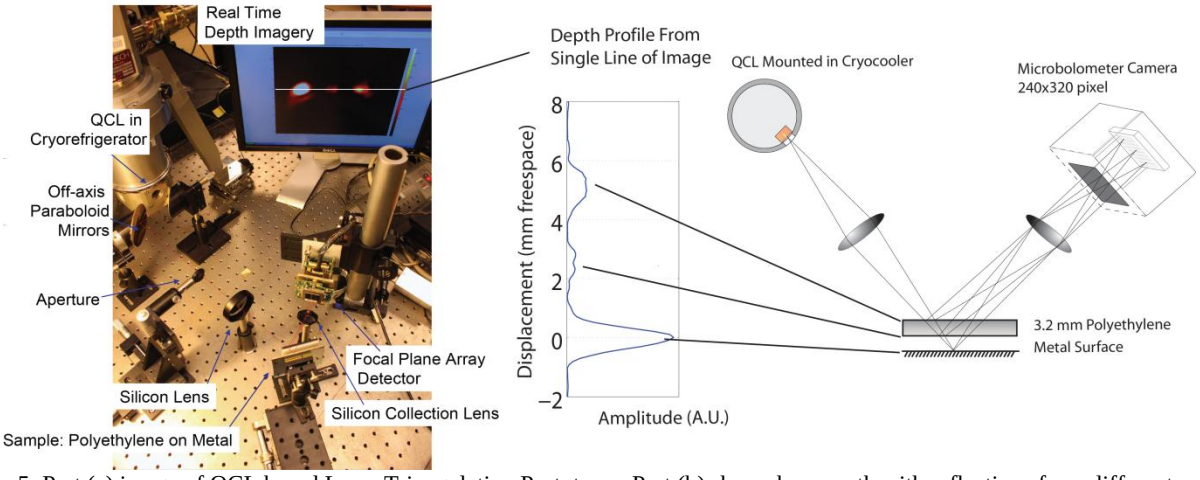

Figure 5: Part (a) image of QCL based Laser Triangulation Prototype. Part (b) shows beam path with reflections from different surfaces of the sample being focused to different positions on the focal plane array.

An obvious improvement to this system would be the use of cylindrical optics to generate a "line" shaped beam, thereby giving a full 2D image – a lateral dimension and a depth dimension. Using this technology, applications targeted by terahertz pulsed imaging could be explored. The benefit of this technology over terahertz pulsed imaging is the large increase in imaging speed: a full 2D tomographic image would be generated at >20 Hz. This would have benefits in the non-destructive imaging applications such as dielectric coating thickness monitoring.

3.3 Single element confocal imaging

A simple confocal imaging system, based on the compact cryocooler of Figure 2 (b), housing a 1.8 THz QCL with an average power of < 1 mW. is shown in Figure 6. Here the laser beam is focused

onto a sample using a optic (an 4.5 cm f/4 off-axis parabolic mirror in this case). Light which is back reflected from an interface in a sample at the focal point is focused with the optic on to an aperture, with the transmitted light being detected. The object is scanned in xyz through the focus of the beam, where any perturbation within this volume leads to a reflection. For objects outside the focal volume, small perturbations reflect small amounts of light. This allows a perturbation at the focal point of the beam to be distinguished from a perturbation outside the focal point i.e. depth resolution. In this setup, a 4 K cooled Silicon bolometer (IRLabs) is used.

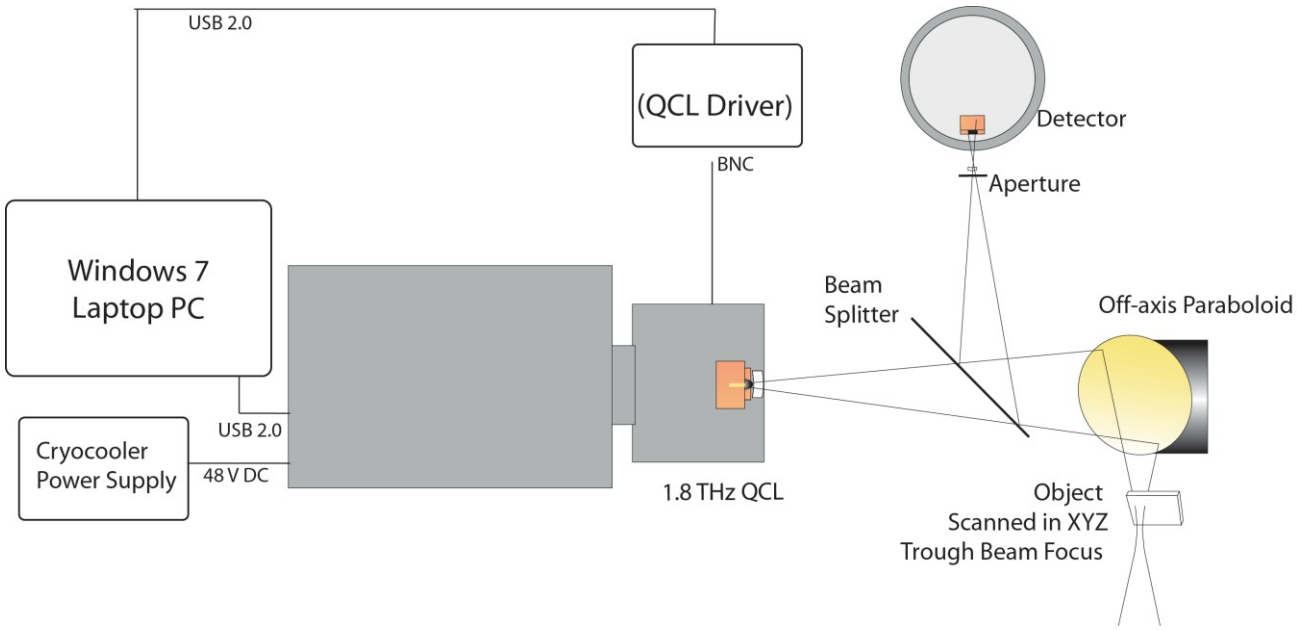

Figure 6. Confocal imaging setup: beam from a 1.8 THz QCL is focus using an off-axis parabolic mirror onto a sample. An interface at the focal point will back reflect light, which is refocused onto an aperture. Light passing through the aperture is detected with a silicon bolometer in this case (part b).

Figure 7 parts (a) and (c) show the results from the confocal imaging scan for various depth planes of the object in part (b). The object is a 1/8" piece of high-density polyethylene with a 1 mm metal circle taped on with cellophane tape. Part (a) shows the image planes in 3D space while part (c) shows all the image planes laid flat. When the object is scanned through the focus of the beam (approximately Z=2 mm), the metal circle is resolved, as well as the partial disbond of the cellophane tape and the edge of the cellophane tape. When the object is scanned out of the focus of the beam (z = 8 mm), only spurious reflections from the metal and disbond are apparent. This experiment was done to quickly verity the xyz scanning stage and the operation of the 1.8 THz laser with the detector system. The more complicated laser triangulation experiment will be performed over the next period.

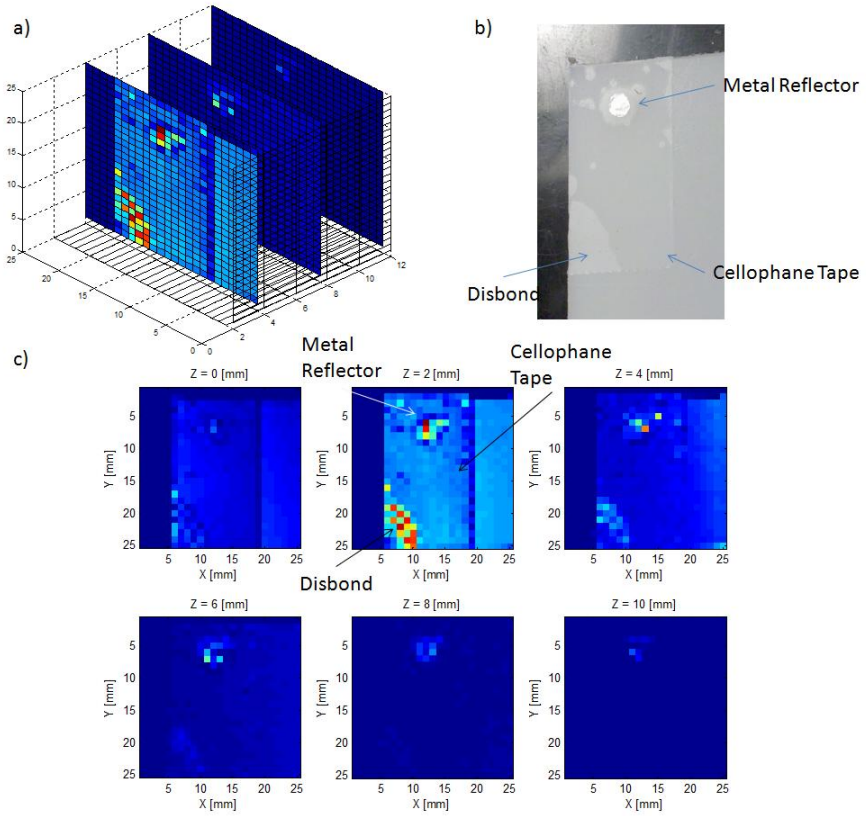

Figure 7. Results from confocal imaging experiment. Part (a) shows scans at various depths arranged in 3D, while part (c) shows the same image planes laid flat on the page. Object being scanned is a 1/8" HDPE piece with metal reflecting dot, and polymer tape.

REFERENCES

[1] L. Li, L. Chen, J. Zhu *et al.*, "Terahertz quantum cascade lasers with> 1 W output powers," Electronics Letters, 50(4), 309-311 (2014).

[2] S. Fathololoumi, E. Dupont, C. W. I. Chan *et al.*, "Terahertz quantum cascade lasers operating up to ~200 K with optimized oscillator strength and improved injection tunneling," Opt. Express, 20(4), 3866-3876 (2012).

[3] A. W. M. Lee, and Q. Hu, "Real-time, continuous-wave terahertz imaging by use of a microbolometer focal-plane array," Optics Letters, 30(19), 2563 - 2565 (2005).

[4] N. Oda, H. Yoneyama, T. Sasaki *et al.*, "Detection of terahertz radiation from quantum cascade laser using vanadium oxide microbolometer focal plane arrays." 6940, 69402Y-12.

[5] Q. Hu, B. S. Williams, S. Kumar *et al.*, "Resonant-phonon-assisted THz quantum-cascade lasers with metal-metal waveguides," Semiconductor Science and Technology, 20(7), 228 - 36 (2005).

[6] B. Williams, S. Kumar, H. Callebaut *et al.*, "Terahertz quantum-cascade laser at 100 m using metal waveguide for mode confinement," Applied Physics Letters, 83(2124), (2003).

[7] A. W. M. Lee, Q. Qin, S. Kumar *et al.*, "High-power and high-temperature THz quantum-cascade lasers based on lens-coupled metal-metal waveguides," Optics Letters, 32(19), 2840 - 2 (2007).

[8] T. Ishi, T. Sudou, N. Oda *et al.*, "Improved image quality of terahertz transmission microscope: Example of graphene film observation." 1-2.

[9] F. Blais, "Review of 20 years of range sensor development," Journal of Electronic Imaging, 13(1), 231-243 (2004).

[10] Micro-Epsilon, [Laser Triangulation Displacement Sensors] Micro-Epsilon, Raleigh, NC(2009).
[11] W. Pastorius, [Triangulation sensors: An overview] InTech, FindArticles.com, (2001).
[12] J. P. Peterson, and R. B. Peterson, "Laser triangulation for liquid film thickness measurements through multiple interfaces," Appl. Opt., 45(20), 4916-4926 (2006).
[13] M. Rioux, F. Blais, J. Beraldin *et al.*, "Range imaging sensors development at NRC Laboratories." 154-160.
[14] R. G. Dorsch, G. Häusler, and J. M. Herrmann, "Laser triangulation: fundamental uncertainty in distance measurement," Appl. Opt., 33(7), 1306-1314 (1994).
[15] A. W. M. Lee, B. S. Williams, S. Kumar *et al.*, "Real-time imaging using a 4.3-THz quantum cascade laser and a 320 x 240 microbolometer focal-plane array," IEEE Photonics Technology Letters, 18(13), 1415 - 1417 (2006).